Research Article

Open Access

Marko Klobučar, Sanja Dević Pavlić, Iris Car, Neda Smiljan Severinski,
Tamara Tramišak Milaković, Anđelka Radojčić Badovinac*±, Sandra Kraljević Pavelić*±

Mass spectrometry-based glycomic profiling of the total IgG and total proteome N-glycomes isolated from follicular fluid

Abstract: Couples with infertility issues have been assisted by *in vitro* fertilization reproduction technologies with high success rates of 50-80%. However, complications associated with ovarian stimulation remain, such as ovarian hyperstimulation. Oocyte quality is a significant factor impacting the outcome of *in vitro* fertilization procedures, but other processes are also critical for fertilization success. Increasing evidence points to aberrant inflammation as one of these critical processes reflected in molecular changes, including glycosylation of proteins. Here we report results from a MALDI-TOF-MS-based glycomic profiling of the total IgG and total proteome N-glycomes isolated from the follicular fluid obtained from patients undergoing fertilization through either (1) assisted reproduction by modified natural cycle or (2) controlled ovarian stimulation (GnRH antagonist, GnRH Ant) protocols. Significant inflammatory-related differences between analyzed N-glycomes were observed from samples and correlated with the ovarian stimulation protocol used in patients.

Keywords: *In vitro* fertilization; inflammation; glycoproteins; follicular fluid glycome; MALDI mass spectrometry.

Introduction

Human reproduction has been acknowledged as a rising public health concern due to the increasing number of couples with conception difficulties. Despite continuous research and development in the field of assisted reproduction technologies (ART), success rates and the understanding of molecular mechanisms underlying this biological process may still be improved [1]. ART success rates are relatively high (50-80%), and complications associated with ovarian stimulation have been decreasing in previous years. However, the occurrence of certain complications associated with ovarian stimulation, such as ovarian hyperstimulation syndrome, remains [2].

Oocyte quality is a critical factor for successful *in vitro* fertilization (IVF). The development of non-invasive methods has improved the assessment of oocyte quality which may contribute to further improvement of ART and fertilization success rate. The oocyte microenvironment comprises of follicular fluid (FF) and somatic cells within the follicle. This environment significantly impacts the quality of oocytes and their development [3]. FF is a complex mixture of hormones, enzymes, cytokines, and other proteins secreted mainly by granulosa cells [4]. Besides oocyte and granulosa cells, the ovarian follicle also contains theca cells in the follicle's external layer. These cells and oocytes are involved, through an intricate interaction, regulate all processes related to follicular differentiation and fertilization [5]. The FF also contains many plasma components that have passed the blood-

*Corresponding authors: Anđelka Radojčić Badovinac, University of Rijeka, Department of Biotechnology, Centre for high-throughput technologies, Radmile Matejčić 2, 51000 Rijeka, Croatia, E-mail: andjelka@biotech.uniri.hr; **Sandra Kraljević Pavelić,** University of Rijeka Faculty of Health Studies, Viktora Cara Emina 5, 51000 Rijeka, Croatia, E-mail: sandrakp@uniri.hr
Marko Klobučar, Iris Car, University of Rijeka, Department of Biotechnology, Centre for high-throughput technologies, Radmile Matejčić 2, 51000 Rijeka, Croatia
Sanja Dević Pavlić, University of Rijeka, Department of Medical Biology and Genetics, Faculty of Medicine, B. Branchetta 20, 51000 Rijeka, Croatia
Neda Smiljan Severinski, Tamara Tramišak Milaković, Department of Obstetrics and Gynaecology, Clinical Hospital Centre Rijeka, Cambierieva 17/5, 51000 Rijeka, Croatia
Anđelka Radojčić Badovinac, University of Rijeka, Department of Medical Biology and Genetics, Faculty of Medicine, B. Branchetta 20, 51000 Rijeka, Croatia
± Equal contribution

follicular barrier [6]. The FF content is continuously changing due to the constant secretion and utilization of specific components by follicular cells, reflecting the physiological or pathological status [6,7]. Furthermore, successful physiological folliculogenesis and ovulation requires an adequate inflammatory response [8,9]. Particularly, a balance between pro and anti-inflammatory processes is required while, the release of gonadotropins during the menstrual cycle causes inflammation and consequent follicle rupture and ovulation [10,11]. Whereas, pathological pro-inflammatory conditions, such as those observed in obesity or polycystic ovary syndrome, have a negative effect on the ovulation process [12,13]. Similarly, controlled ovarian stimulation (COS) is often used in ART procedures, and relies on induced hormonal activation of systemic inflammatory processes [14,15]. Several studies have confirmed a rise in inflammatory cytokines, CRP, and other markers of inflammation in patients subjected to different COS protocols, pointing to an enhanced inflammatory response during ovulation stimulation [16–18]. Inflammation is a complex process extensively involving a plethora of biological processes and molecules [19]. Among them, glycoproteins and glycans have been growingly acknowledged in immune response modulation. In particular, proper glycosylation of glycoproteins plays a pivotal role in the regulation of normal physiological processes [20], and aberrant glycosylation of glycoproteins, i.e., changes in the glycomes of individuals or an entire set of glycosylated proteins, has been associated with various pathological states, including inflammation [21]. Glycosylation of proteins and other biomacromolecules is precisely regulated by enzyme-directed processes that involve linkage of the monosaccharide units to produce glycans, which are eventually covalently attached to protein backbones to form glycoproteins [22]. The entire repertoire of glycans associated with a particular protein, cell or tissue is denoted as 'glycome', systematically studied within the field of glycomics [23]. As glycosylation is influenced by numerous genetic and environmental factors, the resulting glycomes reflect an organism's physiological state and its alternations [24]. There are two major types of protein glycosylation, the N- and O- linked glycosylation. The N-linked glycosylation refers to the attachment of a glycan to a nitrogen atom of asparagine or arginine side chains on a peptide backbone, while the O - linked type involves the glycan attachment on an oxygen atom of serine and threonine side chains [25].

Immunoglobulin G (IgG) is the most abundant glycoprotein, antibody class, in human circulation, which occupies a central role in the immune system [26]. IgG is represented by the four structurally similar subclasses IgG1, IgG2, IgG3, and IgG, of which IgG 1 accounts for up 70% of the total IgG. IgG is a tetrameric N- glycoprotein consisting of two identical heavy 50 kDa (H) and 25 kDa light (L) chains linked together by inter-chain disulphide bonds [27]. It contains two highly conserved N-linked glycosylation sites at asparagine 297, on the fragment crystallizable (Fc) part located between two constant domains (CH2 and CH3 domains) of molecule heavy chains. Also, up to 25 % of circulating IgGs contain additional N-glycosylation sites formed as a result of somatic hypermutations on the molecule fragment antigen-binding (Fab) region [28]. Apart from the well-known influence of IgG conserved N-glycans on subtle changes in the quaternary structure of the molecule Fc region, recent evidence suggests that alternations in the IgG N–glycome are involved in modulation of inflammatory response [29]. The latter is particularly emphasized in extent of antibody sialylation and core fucosylation [30]. For instance, it was shown that a lower degree of sialylation and fucosylation of IgG N-glycans increases the molecule ability to induce antibody-dependent cell-mediated cytotoxicity (ADCC) [31,32]. In line with this, accumulating evidence indicates that the alternations in the N-glycomes of the total proteome isolated from complex biological samples (plasma/serum or tissues) reflects the status of inflammation, or inflammatory disease progression that is frequently associated with specific types of glycoforms sialylation [33,34].

Due to increasing evidence of aberrant inflammation being associated with the alteration of normal ovarian follicular dynamics and infertility [8], here we present a MALDI-TOF-MS-based glycomic profiling of the total IgG and total proteome N-glycomes isolated from FF samples from patients undergoing assisted reproduction by modified natural cycle (MNC) or controlled ovarian stimulation (COH; GnRH antagonist, GnRH Ant) protocols. Several significant inflammatory-related differences between analyzed N-glycomes were observed and varied according to the employed ovarian stimulation protocol.

Materials and methods

Patients

In the study, a total of 20 FF samples were included from 20 patients undergoing assisted reproduction at the Department for Human Reproduction at the Clinic of Obstetrics and Gynaecology, Clinical Hospital Centre Rijeka, Croatia. All women included in the study were

Table 1: Clinical characteristics of the patients included in the study.

Hormonal stimulation	Stimulation protocol	N	Age		No of retrieved oocytes per patient	
			mean ± SD	p	mean ± SD	p
Modified natural cycle (MNC)*	hCG	10	34,2±2,7	0,12	0,8±0,4	<0,01
Controlled ovarian stimulation (COH)*	FSH+GnRH antagonist+hCG	10	37,1±4,9		4,4±2,4	

According to the The ISMAAR proposal on terminology for ovarian stimulation for IVF.

normally ovulatory, between 29 and 44 years of age and with similar referral diagnoses for ART procedures. Patients with diagnosed endometriosis, hyperprolactinemia or polycystic ovarian syndrome (PCOS) were excluded. All included patients were divided into two different groups, according to the applied ovarian stimulation protocol: modified natural cycle group (MNC) (n=10) and controlled ovarian stimulation group (COH; GnRH antagonist, GnRH Ant) ovarian stimulation protocols (n=10) (Table 1.) [35]. The choice of treatment protocol (MNC or COH) was decided after discussion with the couple, taking into account their wishes and clinical characteristics, such as hormonal status, previous pregnancies and ART treatments. In the MNC group all patients were treated with human chorion gonadotrophin (hCG; 5000 IU i.m.) 34 – 36 hours prior to the oocyte aspiration to enable precise triggering of ovulation and thus increased oocyte yield. In the COH group, patients were stimulated with gonadotropin-releasing hormone (GnRH) antagonist combined with FSH. All patients in this group also received hCG (5000 IU i.m.) 34 – 36 hours prior to the oocyte aspiration.

Ethical approval: The research related to human use has been complied with all the relevant national regulations, institutional policies and in accordance the tenets of the Helsinki Declaration, and has been approved by the Ethics Committee of the Clinical Hospital Centre Rijeka (Ur.br. 2170-29-02/1-14-2; July, 11th 2014).

Informed consent: Informed consent has been obtained from all individuals included in this study

Collection of FF samples

Each FF sample was aspirated from the dominant follicle under transvaginal ultrasound guidance. FFs were only included in the study if they did not contain any visible traces of blood. In the COH group, only the fluid from the first aspirated follicle of each patient was carefully collected to avoid blood contamination. The FF was centrifuged at 500 × g for 10 min at 4 °C. The supernatant was transferred and centrifuged at 2000 x g for 30 min at 4 °C to remove cellular debris, then aliquoted and frozen at -20 °C for later analysis.

Purification of the immunoglobulin G (IgG) and isolation of total proteome from the FF

The total IgG was purified from the FF by using Protein G-agarose (Sigma Aldrich, USA) according to the manufacturer instructions. Briefly, 100 µl of the FF was diluted 10x in 20 Mm NaH2PO4 (pH 7.0; Sigma Aldrich, USA) and incubated with 50 µl of homogenous Protein G-agarose suspension overnight at 4 °C. After incubation, the remaining FF supernatant, which contained FF total proteomes separated from the main IgG fraction, was stored at -80°C, while the agarose beads with bound IgG were first washed with 3x 200 µl of 20 Mm NaH2PO4 followed by 5x 200 µl of 20 mM NaH2PO4/ 150 Mm NaCl (pH 7.0; SigmaAldrich, USA) to remove non-specific binding. The bound IgG was released from the protein G-agarose by incubation in 100 µl of 100 mM HCl (SigmaAldrich, USA) for 5 min on RT. The supernatant containing released FF IgG was neutralised by addition of 20 µl of 500 mM NaOH (SigmaAldrich, USA). The isolated FF IgG and FF total protein concentrations were determined by using Qubit ™ quantitation platform (Invitrogen, USA). To assess the purity of isolated FF IgG and measured concentrations of isolated IgG and FF total proteomes, the amounts of each sample corresponding to 3 µg of FF IgG and to 50 µg of FF total proteomes were subjected to 10% SDS-PAGE at 110V for 1.5 h (Supplementary Figure).
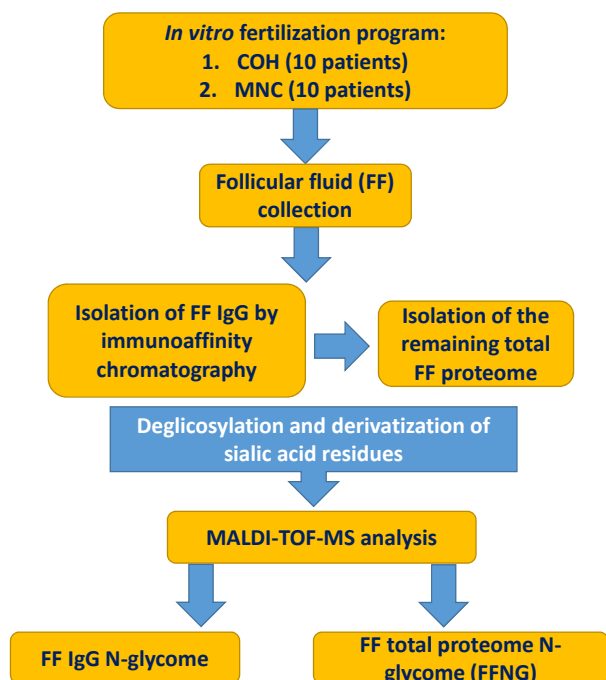
Figure 1: Experimental workflow applied for isolation and analysis of follicular fluid (FF) IgG N-glycome and FF total proteome N-glycome from 10 patients in the modified natural cycle (MNC group) and 10 patients subjected to the controlled ovarian hyperstimulation procedure (COH group). MALDI-TOF-MS, matrix assisted laser desorption ionization time-of-flight mass spectrometry.

Peptide N-glycanase F (PNGaseF) release of N-glycans from FF purified IgG and FF total proteomes

The FF-purified IgG and total proteomes were deglycosylated as described previously with minor modifications [36]. Briefly, prior to enzymatic release of N-linked glycans, equal amounts of purified FF IgG corresponding to 3 µg of isolated proteins were dried in vacuum by a vacuum concentrator (ThermoFisher, USA). Dried purified FF IgG samples were then re-suspended in 10 µl of 5x PBS (Sigma Aldrich, USA) which was followed by addition of 20 µl of 2 % SDS (BioRad, USA) to each sample. The samples were then incubated on 60°C for 30 min. After incubation, 12 µl of PNGaseF release mixture (1:1 4% NP-40: 5x PBS containing 0.75 units of PNGase F, Promega USA) was added to each sample which was followed by an 18 h incubation at 37°C. Similarly, the same amount of remaining FF samples corresponding to 70 µg FF total proteomes were precipitated overnight in 4 volumes of ice-cold acetone (at -20°C; Sigma Aldrich). After precipitation of proteins, the samples were resuspended in 12 µl with 5x PBS followed by addition of 12 µl of 2% SDS

to each diluted sample. The samples were then incubated for 30 min at 60°C. Afterwards, 12 µl of PNGaseF release mixture was added to each sample which was followed by incubation of samples for 18h at 37°C. The released FF purified IgG and FF total proteomes N-glycans were stored at -80°C prior to ethyl-esterification procedure.

Ethyl-esterification and purification of released N-linked glycans

The released N-linked glycans originating from FF purified IgG and FF total proteomes were subjected to ethyl esterification procedure to stabilize the sialylated glycan species during MALDI ionisation process. This procedure enables distinction between α2,3- and α2,6- linked sialic acid (NeuAc) residues by MALDI-TOF-MS analysis as well [37]. Briefly, 1 µl of released N-linked glycan samples 20 µl derivatization reagent (250mM 1-ethyl-3-(3-dimethylaminopropyl)carbodiimide(EDC), 500 mM hydroxybenzotriazole (HoBt) in ethanol; Sigma Aldrich, USA) was added followed by incubation of samples at 37°C for 1h. After incubation, 20 µl of ice-cold acetonitrile (ACN) was added to each sample and left at - 80°C for 15 min. The resulting ethyl esterified N-glycan samples were then subjected to purification by cotton hydrophilic interaction liquid chromatography (HILIC)-solid phase extraction (SPE), as described previously [38]. Cotton filled micropipette tips were equilibrated and conditioned by pipetting 3x 20µl mQ H_2O and 10 µl 85% ACN, respectively. Samples were loaded by pipetting 20 times each through the SPE tips, after which the tips were sequentially washed 3x with 20 µl 85% ACN 1% TFA and 3x with 20 µl 85% ACN. N-glycans were eluted in 20 µl mQ H_2O (Millipore, USA) and dried in a vacuum concentrator (ThermoFisher, USA). Afterwards, the N-linked glycans were re-dissolved in 2 µl of ultrapure water (Millipore, USA), of which 1 µl was mixed with 1 µl of matrix solution (5 mg/ml Super-DHB, 1mM NaOH in 50% ACN; Sigma Aldrich) and spotted on the MTP AnchorChip 384 BC MALDI target (Bruker Daltronics, Bremen, Germany). Samples were then recrystallized by addition of 0.2 µl ethanol to each spot.

Mass spectrometry analysis and data processing

Mass spectrometric measurements of the FF-purified IgG and FF total proteome N-linked glycans, were performed on UltraflexExtreme MALDI – TOF/ TOF instrument (Bruker, Bremen, Germany) equipped with

Table 2: The list of identified N-glycan compositions and their normalized relative abundances (expressed as means ± SD; %) in the FF IgG N-glycomes of the MNC and COH groups of patients. The pairwise differences in individual glycans relative abundances between analyzed groups were considered significant at the p<0,05 (Mann-Whitney U test). Glycan compositions were assigned and associated mass errors were calculated by using GlycoMod platform (29) (http://web.expasy.org/glycomod/) with mass tolerance set to 0.2 Da. Abbreviations: H- hexose; N- N-Acetylhexosamine; F- fucose; E- α 2,6-linked sialic acid; L- α 2,3-linked sialic acid; MNC- group of patients subjected to modified natural cycle stimulation protocol; COH- group of patients subjected to GnRH Ant stimulation protocol.

Glycan composition		Normalized glycan relative abundance (%) ±SD (%)		p- value
		MNC	COH	
Complex afucosylated diantennary compositions	H4N4	1,202±0,379	1,127±0,464	0,878
	H5N4	1,140±3,406	1,081±0,388	0,818
	H4N5	0	0,666±0,010	-
	H5N5	0	0,554±0,028	-
Complex fucosylated diantennary compositions	H3N4F1	9,767±2,882	8,056±3,049	0,557
	H4N4F1	37,634±	34,077±4,837	0,925
	H3N5F1	1,508±0,284%	1,634±0,513	0,204
	H5N4F1	25,890±3,902	27,716±3,277	0,026
	H4N5F1	3,997±0,669	4,720±1,064	0,021
	H5N5F1	1,605±0,233	1,763±0,315	0,034
Complex afucosylated and sialylated diantennary compositions	H4N4L1	0	1,049±0,005	-
	H5N4E1	0,409±0,018	0,658±0,245	0,345
	H5N5E1	0,499±0,089	0,442±0,104	0,820
	H5N4E2	0,501±0,202	0,347±0,056	0,323
	H5N5E2	0	0,232±0,072	-
Complex fucosylated and sialylated diantennary compositions	H4N4F1E1	2,760±0,989	2,712±0,920	0,689
	H5N4F1E1	9,047±2,571	9,574±1,868	0,225
	H4N5F1E1	0,374±0,028	0,409±0,083	0,306
	H5N5F1E1	1,885±0,176	1,644±0,367	0,607
	H5N4F1E2	0,968±0,322	0,714±0,164	0,186
	H5N5F1E2	0,815±0,165	0,827±0,290	0,457

a smartbeam-II™ laser and controlled by Flexcontrol 3.4 software. The 25 kV acceleration voltage was applied with 140 ns extraction delay. Prior to mass spectrometry measurements, the instrument was externally calibrated using a six-point peptide calibration standard (Bruker, Bremen, Germany) with additional internal correction performed by flexControl software (Bruker, Bremen, Germany). The MALDI-TOF-MS spectra were acquired in the reflectron positive ion mode in the 900-4500 m/z range with total of 10000 laser shots at 2000 Hz accumulated per spectra and 200 shots per spot. The MS measurements of each sample were performed in four technical replicates, and all spectra were obtained from Na⁺ adduct ions. All spectra were acquired by flexControl software

(Bruker, Bremen, Germany). The raw MS spectra were processed by flexAnalysis 3.0 software (Bruker, Bremen, Germany). Only signals with signal-to-noise value ≥ 6 were considered for further evaluation. N-linked glycan compositions were assigned using GlycoMod [39] (http://web.expasy.org/glycomod/) platform with mass tolerance set to 0.2 Da. In addition, monoisotopic masses of glycans containing sialic acids were subtracted for 28 Da for each ester and increased for 18 Da during GlycoMod search. The N-glycan compositions (Table 2 and 3; Supplementary Tables 1-6) and structures (N-glycan cartoons displayed in Figures 2-5) used in this study were presented according to the recommendation by the Consortium for functional glycomics [40].

Table 3: The list of identified N-glycan compositions and their normalised relative abundances (expressed as means ±SD; %) in the FFNGs of the MNC and COH groups of patients. The pairwise differences in individual glycans relative abundances between analyzed groups were considered significant at p<0,05 (Mann-Whitney U test). The glycan compositions were assigned and the associated mass errors were calculated by using GlycoMod (29) (http://web.expasy.org/glycomod/) platform with mass tolerance set to 0.2 Da. Abbreviations: H- hexose; N- N-Acetylhexosamine; F- fucose; E- α 2,6-linked sialic acid; L- α 2,3 -linked sialic acid; MNC- group of patients subjected to modified natural cycle stimulation protocol; COH- group of patients subjected to GnRH Ant stimulation protocol.

Glycan composition		Normalized glycan relative abundance (%) ±SD (%)		p-value
		MNC	COH	
Oligomannose compositions	H5N2	0,206 ± 0,096	0,191± 0,052	0,676
	H6N2	0,703± 0,230	0,585± 0,110	0,163
	H7N2	0,211± 0,078	0,180± 0,048	0,314
	H8N2	0,491± 0,158	0,368± 0,111	0,060
	H9N2	0,897± 0,277	0,672± 0,205	0,052
Hybrid compositions	H10N6	0,069± 0,014	0,077± 0,021	0,613
	H15N3	0	0,055± 0,011	-
Complex afucosylated compositions	H4N4	0,125± 0,078	0,211± 0,018	0,125
	H4N5	0,174± 0,011	0,166± 0,078	0,900
	H5N4	0,183± 0,023	0,165± 0,067	0,807
Complex fucosylated and asialylated compositions	H3N4F1	0,603± 0,121	0,248± 0,108	0,026
	H4N4F1	1,336± 0,053	0,494± 0,181	0,022
	H3N5F1	0,172± 0,061	0,175± 0,065	0,972
	H5N3F1	0,260± 0,044	0,241± 0,029	0,753
	H5N4F1	1,003± 0,176	0,452± 0,287	0,053
	H4N5F1	0,288± 0,099	0,266± 0,016	0,654
	H5N5F1	0,225± 0,076	0,155± 0,037	0,081
	H8N4F1	0,264± 0,112	0,285± 0,086	0,432
	H7N6F1	0,125± 0,032	0,092± 0,032	0,035
Complex afucosylated and sialylated compositions	H4N3E1	0,260± 0,052	0,228± 0,038	0,129
	H4N4E1	0,241± 0,051	0,211± 0,038	0,144
	H5N4L1	0,210± 0,032	0,188± 0,048	0,660
	H5N4E1	6,101± 1,251	5,745± 1,574	0,579
	H4N5E1	0,210± 0,014	0,191± 0,056	0,556
	H5N5E1	0,361± 0,081	0,366± 0,117	0,920
	H5N4L2	0,270± 0,140	0	-
	H5N4E1L1	3,555± 0,737	3,887± 1,349	0,500
	H5N4E2	69,409± 4,683	73,344± 5,162	0,086
	H6N5E1	0,421± 0,075	0,349± 0,101	0,085
	H5N4F1E1L1	0,471± 0,076	0,391± 0,097	0,052
	H4N7E1	0,125± 0,017	0	-
	H6N5E1L1	0,359± 0,074	0,342± 0,129	0,727
	H6N5E2	0,354± 0,082	0,277± 0,058	0,027

Continued Table 3: The list of identified N-glycan compositions and their normalised relative abundances (expressed as means ±SD; %) in the FFNGs of the MNC and COH groups of patients. The pairwise differences in individual glycans relative abundances between analyzed groups were considered significant at p<0,05 (Mann-Whitney U test). The glycan compositions were assigned and the associated mass errors were calculated by using GlycoMod (29) (http://web.expasy.org/glycomod/) platform with mass tolerance set to 0.2 Da. Abbreviations: H- hexose; N- N-Acetylhexosamine; F- fucose; E- α 2,6-linked sialic acid; L- α 2,3 -linked sialic acid; MNC- group of patients subjected to modified natural cycle stimulation protocol; COH- group of patients subjected to GnRH Ant stimulation protocol.

| Glycan composition		Normalized glycan relative abundance (%) ±SD (%)		p-value
		MNC	COH	
Complex fucosylated and sialylated compositions	H6N5F1E1L1	0,105± 0,034	0,087± 0,018	0,209
	H6N5E1L2	0,198± 0,058	0,241± 0,131	0,354
	H6N5E2L1	2,482± 0,447	2,944± 1,394	0,333
	H6N5E3	0,893± 0,166	0,763± 0,151	0,081
	H7N6E2	0,061± 0,005	0,075± 0,003	0,076
	H6N5F1E1L2	0,091± 0,030	0,079± 0,022	0,341
	H7N6E1L2	0,091± 0,026	0,094± 0,042	0,864
	H7N6E2L1	0,077± 0,018	0,073± 0,035	0,713
	H7N6E1L3	0,053± 0,022	0,070± 0,020	0,473
	H7N6E2L2	0,070± 0,016	0,077± 0,054	0,698
	H7N6E3L1	0,035± 0,011	0,038± 0,022	0,736
	H4N4F1E1	0,168± 0,069	0,102± 0,010	0,150
	H5N4F1L1	0,215± 0,055	0,187± 0,027	0,157
	H4N5F1L1	0,159± 0,055	0,129± 0,031	0,255
	H5N4F1L1	1,010± 0,298	0,609± 0,220	0,035
	H4N4F1L1	0,188± 0,053	0,188± 0,090	0,999
	H5N5F1E1	0,457± 0,110	0,417± 0,100	0,392
	H5N4F1L2	0,196± 0,075	0,260± 0,124	0,255
	H4N6F1E1	0	0,168± 0,053	-
	H5N4F1E2	1,957± 0,567	1,381± 0,401	0,017
	H6N5F1E1	0,135± 0,043	0,107± 0,016	0,089
	H5N5F1E2	0,364± 0,083	0,330± 0,142	0,518
	H6N5F1E2	0,119± 0,032	0,098± 0,015	0,085
	H6N5F1E2L1	1,015± 0,394	0,744± 0,379	0,129
	H6N5F1E3	0,070± 0,023	0,052± 0,012	0,064
	H7N6F1E1L2	0,045± 0,008	0,036± 0,002	0,101
	H7N6F1E1L3	0,029± 0,011	0,028%± 0,008	0,863
	H7N6F1E2L2	0,036± 0,011	0,029± 0,005	0,187
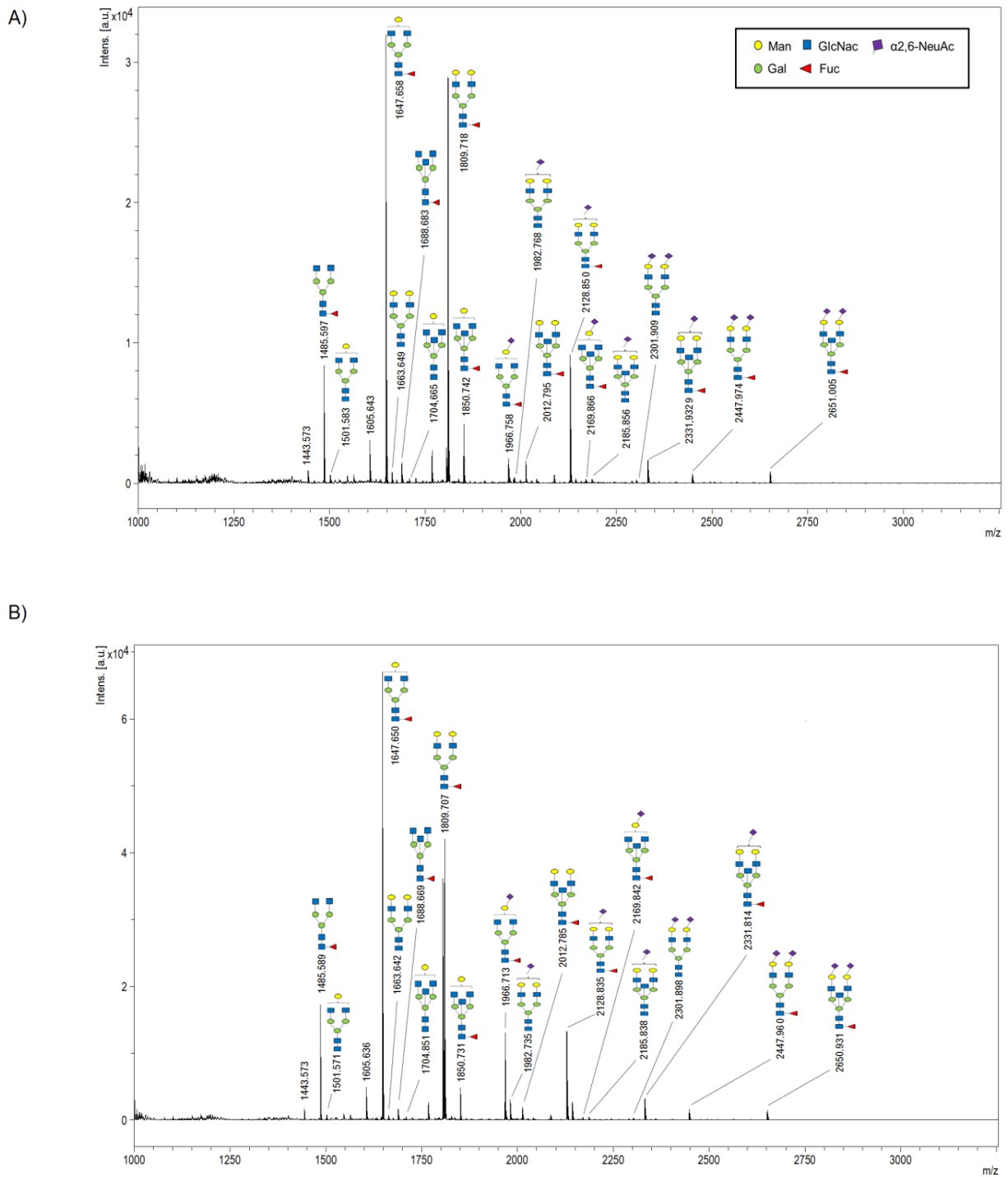
Figure 2: Representative MALDI-TOF-MS spectra of released and derivatised N-glycans (including their monoisotopic masses) obtained from IgG samples isolated from FF of (A) MNC and (B) COH groups of patients. Displayed N-glycan structures are given based on their observed masses and literature [49]. Abbreviations: Man, mannose; Gal, galactose; Fuc, fucose; GlcNac, N-Acetylglucosamine; α 2,6- NeuAc, α 2,6 –linked sialic acid; α 2,3- NeuAc, α 2,3-linked sialic acid.
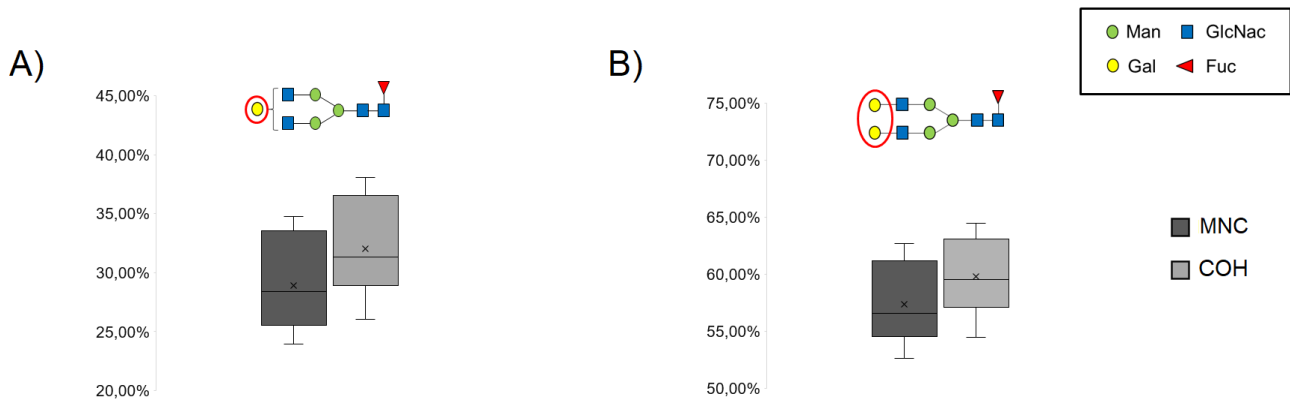
Figure 3: Statistically significant deregulated FF IgG N-glycome derived traits presented as mean±SD (Mann-Whitney U test, p<0,05) between MNC and COH groups of patients. Displayed traits include (A) % of galactosylation and (B) % bigalactosylation of IgG diantennary N-glycans. The minimal N-glycan structure representing each trait is presented in each panel with red circle indicating analyzed features. Abbreviations: Man, mannose; Gal, galactose; Fuc, fucose; GlcNac, N-Acetylglucosamine.
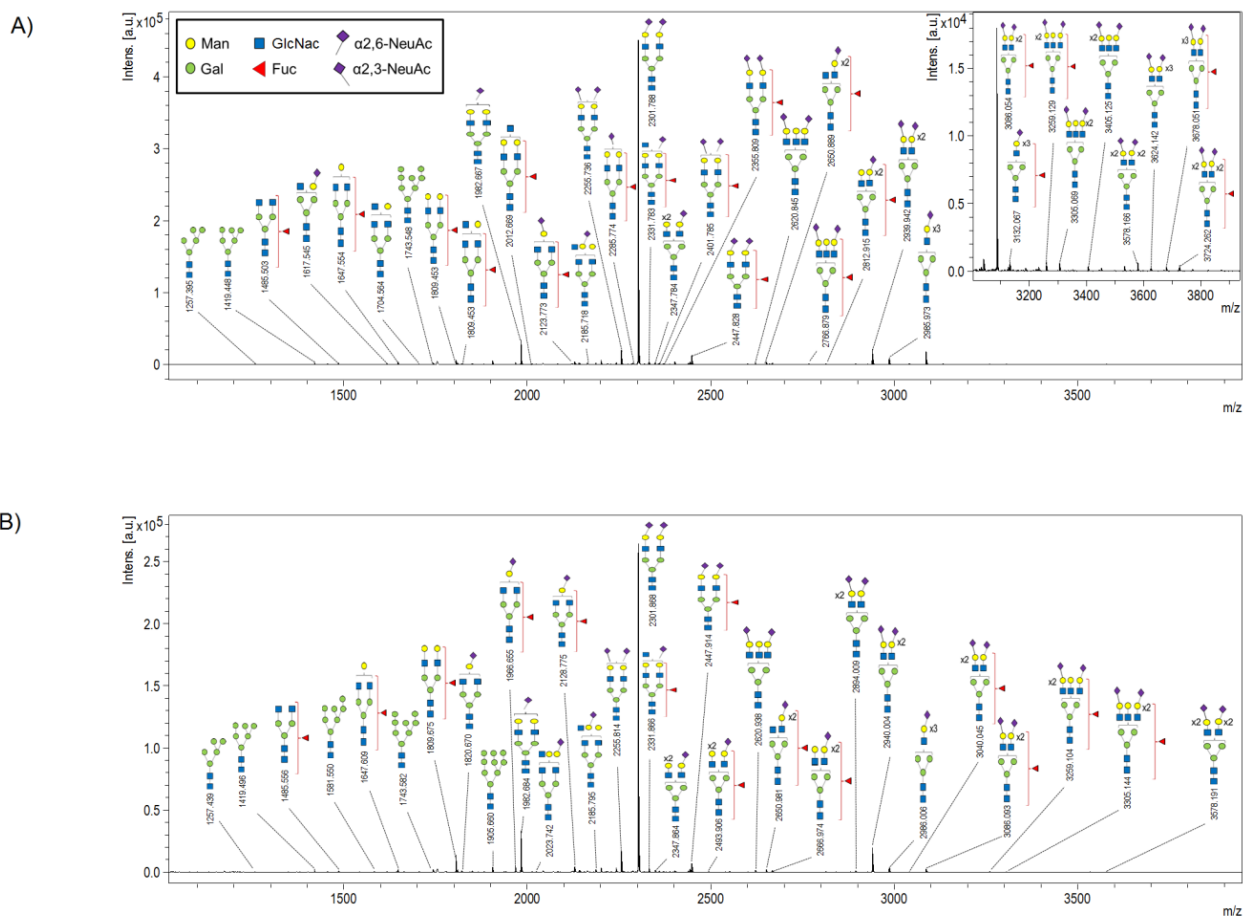

Figure 4: Representative MALDI-TOF-MS spectra of released and derivatised N-glycans (including their monoisotopic masses) obtained from FF total proteomes (FFNG) samples of (A) MNC and (B) COH groups of patients. The displayed N-glycan structures are given based on their observed masses and literature [46]. The magnified view on Figure 1A shows mass spectrum from 3000-3500 m/z region. Abbreviations: Man, mannose; Gal, galactose; Fuc, fucose; GlcNac, N-Acetylglucosamine; α 2,6- NeuAc, α 2,6 –linked sialic acid; α 2,3- NeuAc, α 2,3-linked
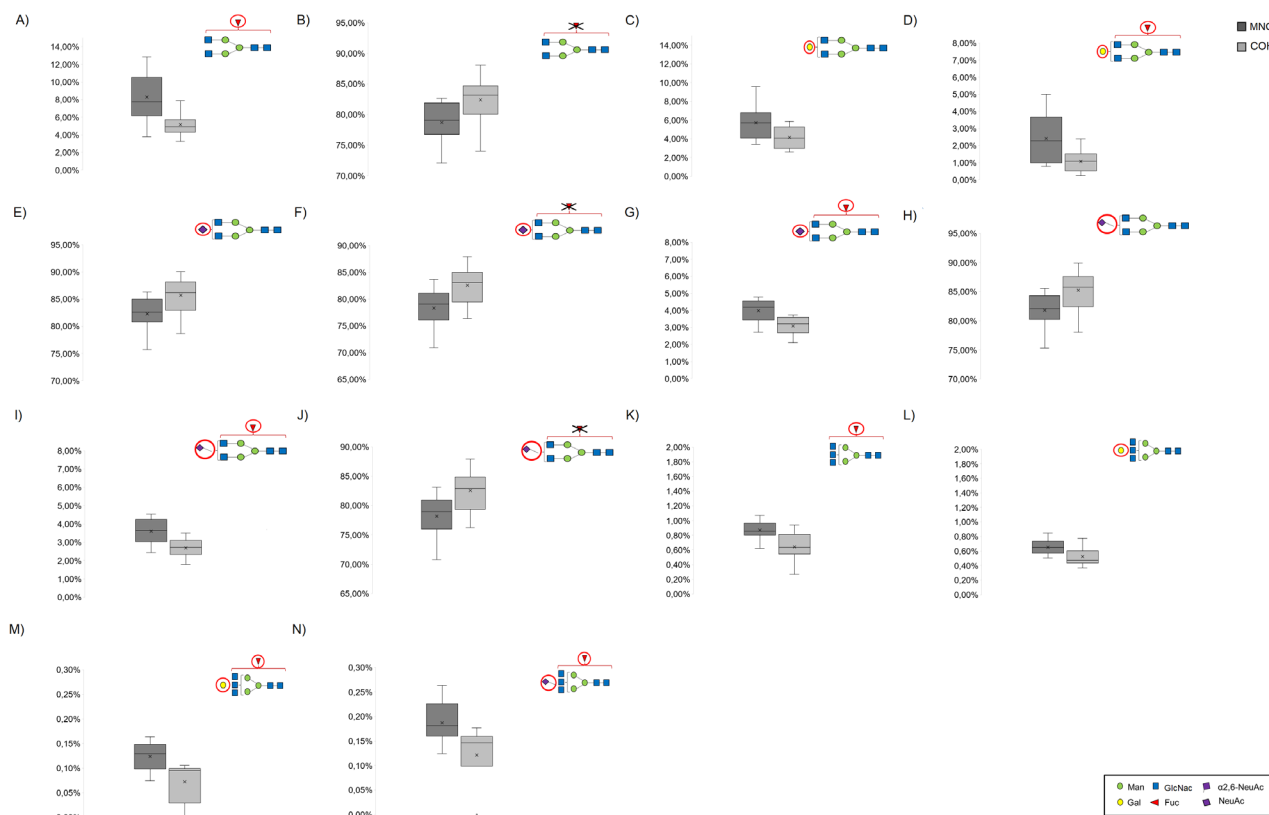
Figure 5: Statistically significant (Mann-Whitney U test, p<0,05) deregulated FFNGs-derived traits presented as mean ±SD between MNC and COH groups of patients. The presented traits are exclusively FFNGs additional traits derived from (A-J) diantennary and (K-N) triantennary complex type N-glycans identified in both analyzed groups. The displayed traits include: (A) % of fucosylated diantennary compositions; (B) % of afucosylated diantennary compositions; (C) % of galactosylation diantennary compositions; (D) % of galactosylation of fucosylated compositions; (E) % of sialylation of diantennary compositions; (F) % of sialylation of afucosylated diantennary compositions; (F) % of sialylation of afucosylated diantennary compositions; (G) % of sialylation of fucosylated diantennary compositions; (H) % of α2,6- sialylation of diantennary compositions; (I) % of α2,6- sialylation of fucosylated diantennary compositions; (J) % of α2,6- sialylation of afucosylated diantennary compositions; (K) % of fucosylated triantennary compositions; (L) % of galactosylation of triantennary compositions; (M) % of galactosylation of fucosylated triantennary compositions and (N) % of α2,6- sialylation of fucosylated triantennary compositions. The minimal N-glycan structure representing each trait is presented in each panel with a red circle that indicates analyzed features. Abbreviations: Man, mannose; Gal, galactose; Fuc, fucose; HexNac, N-Acetylhexosamine; NeuAc, sialic acid; α 2,6- NeuAc, α 2,6 –linked sialic acid.

Data analysis

As glycan signal relative intensities obtained by MALDI-TOF-MS reflect their molar proportions in the sample, the relative abundances (%) of identified N-linked glycans (representing the ratio of individual glycan species to the whole analyzed N-glycan profile) were calculated as the sum of the MS signal intensities of distinct oligosaccharide structure normalized by the sum of the signal intensities for all quantified N- glycans in the each analyzed profile [41]. In addition, the 9 FF IgG and 44 FF total proteome N-glycome derived traits (based on single enzymatic step addition of monosaccharide units) were also calculated in this study. These N-glycome traits reflect identified N-linked glycans compositional features associated with changes in glycosylation pathways and thus provide a more robust approach for biological interpretation of MS-based glycomics results [36]. The derived traits were calculated based on the normalised intensities of identified glycan species bearing distinct features as described previously (the calculations of derived traits are presented in Supplementary Tables 3 and 4) [36,42,43].

Statistical analysis

As part of the data were not normally distributed (Kolmogorov–Smirnov test), the pairwise differences in

the in the relative N-linked glycan abundances and the derived glycan traits were obtained using Mann-Whitney U-test, where p<0.05 was statistically significant. All analyses were performed in Statistica 12. The results of individual N-glycan relative abundances and derived traits analyses were presented as the mean ± standard deviation (SD) in percentages (%).

Results

In this study, the immunoglobulin G was isolated by immunoaffinity chromatography from purified FF from 20 patients subjected to different ovarian stimulation protocols: 10 patients in the modified natural cycle (MNC group) and 10 patients subjected to the controlled ovarian hyperstimulation procedure (COH group). The N-linked glycans derived from IgG molecule (FF IgG N-glycome) and the remaining FF total proteomes (FF N-glycome/FFNG) were enzymatically cleaved and subjected to previously described derivatisation procedure which enables the distinction between α2,3- and α2,6-terminally linked sialic acid residues in the MALDI-TOF-MS spectra [38]. N-glycomes of FF-isolated IgG and total proteomes were analyzed separately by MALDI-TOF-MS (the experimental workflow is depicted in Figure 1).

As MALDI-TOF-MS provides information only on the glycan composition but not of the exact glycan structure, i.e., does not distinguish between different glycan isomers except for the linkage of terminal sialic acids, the FF IgG N-glycans compositions (presented in Table 2 and Supplementary Tables 1, 3 and 5) and structures (displayed as schematics in Figures 2 and 3) were presented based on the observed IgG N-glycans monoisotopic masses, previously well-characterized structures of the IgG N-glycans [44] and confirmation MS/MS experiments of the abundant FF IgG glycan species (data not shown). Importantly, the majority of FF proteins originate from blood which in a high level of similarity in the protein composition between human plasma and the FF [45]. Accordingly, the compositions (presented in Table 3 and Supplementary Tables 2, 4 and 6) and structures (displayed as schematics in Figures 2 and 4) of N-linked glycans, derived from the FFNGs, are given based on their observed monoisotopic masses, previously well-characterized in blood plasma N-glycans [36,46,47] and confirmation MS/MS experiments of the abundant FFNGs N-glycan species (data not shown).

FF IgG N-glycome profiling by MALDI-TOF-MS

The MALDI-TOF-MS profiling of derivatised N-linked glycans isolated from purified FF IgG in both groups of patients yielded a total number of 21 consistently present N-glycan glycoforms, whose normalized intensities were further used for quantitation within the analyzed IgG N-glycome profiles (Table 1; the average monoisotopic masses and proposed compositions of identified derivatised N-glycans in both analyzed groups are presented in Supplementary Table 1). All identified N-glycans were complex diantennary compositions of variable relative abundances (0-35% of the IgG N-glycome profiles; Table 1). Another frequent observation in FF IgG N-glycans was the heptasaccharide core fucosylation. More than 96% of detected glycans possessed this type of modification in both analyzed profiles (Table 2 and Supplementary Table 5), which is commonly observed in N-glycans of IgG derived from biological samples [36,48]. The representative spectra of FF IgG N-glycans from MNC and COH profiles are presented in Figure 2.

The MALDI-TOF-MS based comparative analysis of the individual glycan relative abundances, revealed several significantly deregulated glycoforms between analyzed groups (Table 1). These include core fucosylated and bigalactolysed glycan H5N4F1 and core fucosylated and monogalactolysed glycan H5N5F1, whose levels were significantly elevated (p<0.05) in the COH vs. MNC group (Table 2). Furthermore, additional low abundant N-glycan species representing less than 1% of the total IgG N-glycome profile were also found to be deregulated between the analyzed groups. These include two monogalactolysed (H4N5 and H5N5) and monosialylated (H4N4L1 and H5N5E2) N-glycan compositions, which were only identified in the COH group of patients (Table 2).

The differences between the analyzed FF IgG N-glycomes were calculated and a comparison of the nine IgG N-glycome-derived traits that reflect specific glycan features between two groups of patients was summarized (Supplementary Table 5). The calculations of derived traits were performed based on the normalized intensities of 21 identified N-glycans (Supplementary Table 3). The comparative analysis of FF IgG N-glycome features revealed statistically relevant differences only in the levels of two derived traits between the MNC and COH profiles most likely due to a low number of detected glycans bearing a specific feature. These are galactosylation and bigalactosylation levels of the FF IgG N-glycome, which were both significantly downregulated (p<0.05) in the MNC vs. COH profile (Figure 3A and 3B; Supplementary Table 5). Also, these results are largely derived from the

most abundant significantly deregulated individual galactolysed N-glycan species, for instance N-glycans H5N4F1, H4N5F1 and H5N5F1, between analyzed groups (Table 1). In addition, non-significant alternations in the regulation of several features between analyzed groups were also observed (Supplementary Table 5). The most prominent differences were observed for agalactosylation and bisection levels associated with differential regulation of individual agalactolysed and bisected N-glycan species, where the former were increased, and the latter decreased in the MNC vs COH profile (Supplementary Table 5).

MALDI-TOF-MS comparative analysis of FFNGs

The analysis of MNC and COH FFNGs by MALDI-TOF-MS revealed a total of 61 constant distinct glycoforms, which were subsequently used for quantitation of individual glycans and calculation of the N-glycome-derived traits, as described in the previous section. The average monoisotopic masses of identified N-glycans are presented in Supplementary Table 2. The representative spectra of N-glycans identified in MNC and COH groups are given in Figure 2. The majority of identified glycan compositions were complex type N-glycans representing more than 98% of the total N-glycome profiles in both analyzed groups (Table 3 and Supplementary Table 6). These N-glycans had varying degrees of branching (including bi-, tri- and tetra-antennary compositions) and whose antennae were often terminated with α 2,3- and α 2,6- linked sialic acids (Figure 3; Table 3). In addition, the backbones of detected complex N-glycans were modified to some extent only with a single fucose residue (Figure 3; Table 3). For diantennary compositions it can be hypothesized that fucoses are linked on a glycan heptasaccharide core [49]. On the other hand, in the trianntenarry and tetraantennary composition fucoses are most likely present on the glycan antenna, at least in the most common plasma N-glycoproteins [36,46]. Furthermore, besides the complex type N-glycans, several oligomannose and hybrid compositions were also identified by MALDI-TOF-MS (Figure 3 and Table 3).

The comparative analysis of individual glycan relative abundances by MALDI-TOF-MS revealed relevant differences in regulation of ten N-glycan species between the two analyzed profiles (Table 3). In the MNC group, six N-glycan species showed significantly increased abundances ($p < 0.05$) compared with the COH group: three complex fucosylated asialylated (H3N4F1, H4N4F1 and H7N6F1) and three complex fucosylated sialylated (H6N5E2, H5N4F1L1 and H5N4F1E2) compositions (Table 3). Moreover, two compositions, namely mono- and bisialylated complex N-glycans (H4N7E1 and H6N5E2, respectively) were exclusively identified in the MNC group (Table 3). In contrast, the hybrid composition H15N3 and complex monosialylated fucosylated N-glycan H5N6F1E1 were identified only in the COH group of patients (Table 3). Furthermore, a set of 44 derived N-glycome traits reflecting the differences in the compositional features of detected individual glycans were calculated and compared between FF N-glycomes from two analyzed groups of patients. To provide a comprehensive biological insight into the analyzed N-glycomes changes, the traits were categorized into three groups, which included all identified N-glycans and 41 additional features exclusive to complex type N-glycans (Supplementary Table 6). This mitigates to a certain extent uncertainties observed between analyzed FFNGs as they could be partially attributed to the differential glycoprotein expression and to the changes in extent of individual glycoprotein glycosylation [36]. Additional traits were analyzed separately according to the 'degree of branching' of identified glycans (including diantennary, triantennary and tetraantennary compositions) and to their fucosylation, galactosylation and (linkage specific) sialylation (Supplementary Table 6). The calculations of the derived and additional complex type N-glycan traits are given in the Supplementary Table 4. The comparison between the MNC and COH FFNGs revealed minor, but significant differences, in the regulation of 14 traits, all of which were related only to additional features derived from the identified complex type N-glycans. In the MNC profile, the levels of general fucosylation were found to be significantly increased ($p < 0.05$) for diantennary complex compositions, while the levels of afucosylated diantennary compositions showed reduced regulation in the COH profile ($p < 0.05$; Figure 5 and Supplementary Table 6). Furthermore, the galactosylation levels of diantennary compositions were found to be significantly elevated ($p < 0.05$) in the MNC profile (Figure 5 and Supplementary Table 6), which was accompanied by significantly increased galactosylation ($p < 0.05$) of fucosylated diantennary composition observed also in the MNC profile (Figure 5 and Supplementary Table 6). Concerning the analysis of sialylation of complex diantennary glycans, the significant increases ($p < 0.05$) of general sialylation and sialylation of afucosylated compositions were observed in the COH profile (Figure 5 and Supplementary Table 6). Moreover, significantly elevated levels ($p < 0.05$) of α 2,6- sialylation and more specifically α 2,6- sialylation of afucosylated diantennary compositions were observed also in the COH profile (Figure 5 and Supplementary Table 6). These

observations were all in line with previously described elevated levels of afucosylated diantennary compositions observed in the COH profile. In contrast, the levels of α 2,6-sialylation of fucosylated diantennary compositions were increased significantly ($p < 0.05$) in the MNC profile (Figure 5 and Supplementary Table 6), which is in line with increased fucosylation of diantennary compositions, also observed in the MNC profile. In addition, the analysis of triantennary complex N-glycan features revealed similar trends, as observed for diantennary compositions. For instance, the levels of general fucosylation and galactosylation of triantennary compositions were also found to be significantly increased ($p < 0.05$) in the MNC profile (Figure 5 and Supplementary Table 6). These observations were followed by significantly increased ($p < 0.05$) galactosylation and α 2,6-sialylation levels of fucosylated triantennary compositions, also in the MNC vs NCOH profile (Figure 5 and Supplementary Table 6), which is directly related to increased general fucosylation levels observed for the triantennary compositions in the MNC profile. Interestingly, no significant differences in the regulation of α 2,3- linked sialylation at any level of complexity of analyzed FFNG profiles were observed, although an almost two-fold increase in α 2,3- linked sialylation of fucosylated tetraantennary N-glycans was determined in the MNC vs COH group of patients (Supplementary Table 6).

Discussion

Ovarian follicular maturation is a dynamic process under the control of complex systemic endocrine signalisation and local level control mechanisms [50]. A precisely regulated local inflammatory response is essential for proper folliculogenesis and ovulation [8]. Accordingly, inflammatory misbalances associated with different IVF stimulation protocols can alter normal ovarian follicular dynamics resulting in impaired oocyte quality and negative IVF outcome [15,51,52]. Moreover, evidence supports the association of aberrant inflammation in diverse IVF stimulation protocols and development of various pathological states, including ovarian hyperstimulation syndrome (OHSS) [53]. These processes are involved in maturation of the oocytes and occur within the FF, a dynamic milieu that surrounds the developing oocyte [54]. Apart from various steroid hormones and metabolites, FF contains a large amount of secreted proteins originating both from the blood plasma and oocyte surrounding cells. These proteins reflect the degree of follicle maturation [55,56]. As more than 60% of secreted proteins are

glycosylated, glycosylation changes are associated with disturbed inflammatory homeostasis [21,57] or even infertility [58]. Immunoglobulin G is the most common antibody class in the circulating plasma that contains two conserved N-glycosylation sites at Asn-297 residues on its constant heavy 2 (CH2) domains of fragment crystalible (Fc) region. Besides the two conserved glycosylation sites on the Fc portion of the molecule, 15-20% of circulating IgG also contains additional non-conserved glycosylation sites on the Fab portion [59]. The intra-individual IgG N-glycome is rather stable but it can change rapidly upon disruption of normal physiological conditions, as observed in various diseases and pathological states, including inflammation [33]. Moreover, it is well documented that depending on its Fc glycosylation status, IgG can exert pro- or anti-inflammatory activity by modulating its interactions with the receptors of the immune system [60]. Accordingly, we focused our study on comparative analysis of the (a) N-glycomes in the FF IgG, as one of the most common glycoproteins in the FF [61], and (b) FF N-glycans (FFNGs) obtained from patients that underwent IVF by different stimulation protocols (including modified natural cycle receiving only hCg and GnRH Ant protocol) using a MALDI-TOF-MS approach.

Our results revealed a total of 21 distinct diantennary complex type N-glycans in both groups of patients. These observations are in line with previous studies based on MALDI-TOF-MS where up to 30 different IgG N-glycoforms were found in the human plasma [36]. Also, considering the N-glycan compositions, most of identified N-glycans had a core fucose (more than 96% of identified glycans) and only a minor proportion were modified with α 2-6 sialic acids, which is consistent with previous structural characterization of IgG Fc N-glycans [62]. In addition, only one identified N-glycoform, namely the glycan H4N4L1, contained α 2-3 linked sialic acid (Table 2), most likely corresponding to the glycosylation of the fragment antigen-binding (Fab) antibody portion which contains more processed N-glycans, including alpha 2-3 sialylated structures [59]. The comparative analysis of IgG glycosylation between MNC and COH group revealed minor, albeit significant differences in individual glycan relative abundances (Table 2). These were mostly related to a relative increased abundance of the galactosylated and sialylated N-glycan species in the COH vs MNC group, galactosylated being more pronounced (Table 2). Additional IgG N-glycome comparative analysis of the IgG N-glycome derived trait differences, revealed significantly increased galactosylation accompanied by a significant increase in bigalactosylation in the COH vs MNC group of patients (Figure 3 and Supplementary Table 5). Since we can assume, with a high probability, that the majority

of FF IgG originates from the transfer of blood plasma proteins through the thecal capillaries [56,63], the elevated antibody galactosylation observed in this study might be, at least partially, attributed to the increased systemic levels of oestrogen (E2) concentrations observed during the IVF stimulation protocols treatment [64,65]. It is well known that oestrogen modulates IgG glycosylation by regulating glycosyltransferase activity in antibody-producing cells [66]. Moreover, oestrogen promotes galactosylation of IgG N-glycans, in both genders, by an unknown mechanism [67] and elevated serum IgG galactosylation forms are associated with increased oestrogen concentrations in systemic circulation during pregnancy [68]. Also, it is generally accepted that IgG galactosylation reflects the status of inflammation and contributes to its anti-inflammatory activity [33], as evidenced in various pathological states, including, inflammatory diseases, cancer and chronic inflammation [69]. Furthermore, it is proposed that agalactolysed IgG has a pro-inflammatory role through the activation of several immune system pathways [70]. Indeed, it is known that terminal galactose residues are necessary for addition of sialic acids during enzymatic synthesis of N-glycans, and that the levels of both types of modifications are often highly correlated on a single protein level [71]. Furthermore, increasing evidence suggests that the addition of sialic acid on the IgG N-glycans contributes to its anti-inflammatory activity by an incompletely clarified mechanism [69,72]. Taking all this into account, it is logical to assume that increased IgG galactosylation observed in FF obtained from the COH group of patients is associated with a decreased inflammatory response. However, the expected concomitant increase of galactosylation and sialylation of FF IgG N-glycans was not observed in our study. Recent evidence suggests that IgG terminal galactoses contribute to molecule pro-inflammatory activity via enhancement of its affinity towards FcγR receptors [73] and complement component C1q [74]. Therefore, the role of this modification remains controversial. Moreover, several in-depth comparative proteomic studies of FF revealed increased activation of the complement pathways in FF obtained from GnRH Ant-stimulated vs. modified natural cycle patients [75–77]. The role of increased galactosylation of IgG observed in this study should be therefore, interpreted with caution, until additional comparative glycomic studies between plasma and FF IgG glycosylation accompanied by FF proteomic mechanistic analyses on a larger set of patients have been performed.

In addition, we found 61 individual glycoforms, mainly complex type N-glycans, in both analyzed groups of FFNGs (Table 3). Considering individual glycan compositional features and their relative abundances, the analyzed FFNGs exhibited similarities with the human plasma N-glycome. For instance, the most abundant glycoform detected in both analyzed profiles was the complex diantennary glycan composition H5N4E2, as previously reported in the human plasma N-glycome [46]. This result was expected, as a large amount of secreted proteins in FF originates from the systemic circulation [63]. In addition, both analyzed N-glycome profiles showed a high degree of similarity between their compositional features and relative abundances levels (Table 3 and Figure 4), as additionally reflected in the MALDI-TOF-MS based comparative analysis results of the FF N-glycomes. Importantly, all observed differences between analyzed FFNGs can be partially attributed to differential glycoprotein expression due to different stimulation protocols, as previously observed in the comparative proteomic studies of FF [76,77]. Moreover, effects of the nucleotide sugar precursor donors' availability and the extent of glycosylation of individual glycoproteins on observed FFNG changes, should also not be excluded, since they have not been investigated in the FF so far.

On the individual glycan level, only ten low-abundant complex types of N-glycan species were significantly deregulated between the analyzed groups (Table 3). The most prominent differences were observed for the diantennary fucosylated asialylated (H3N4F1 and H4N4F1) and sialylated (H5N4F1L1 and H5N4F1E2), diantennary and triantennary afucosylated sialylated (H5N4L2 and H6N5E2, respectively) and triantennary fucosylated asialylated (H7N6F1) compositions, where levels were statistically increased in the MNC vs. COH group (Table 3). In addition, the tetraantennary afucosylated sialylated composition (H4N7E1) was also detected only in the MNC group (Table 3).

The core fucosylated diantennary compositions most likely originate from the Fc portion of the FF residual IgG, while the core fucosylated sialylated diantennary compositions are usually linked to other circulating antibodies, such as IgA or IgM [36,78], which were previously identified in FF [79]. On the other hand, diantennary and triantennary afucosylated sialylated (H5N4L2 and H6N5E2, respectively) and triantennary fucosylated asialylated (H7N6F1) compositions are usually confined to the acute phase blood serum derived proteins (APP) [80], which are commonly encountered in FF [81]. Indeed, these N-glycan structures may be linked to the APPs as leucine-rich alpha 2- glycoprotein, alpha-2-macroglobulin, prothrombin and complement components, which we found to be upregulated in FF obtained from patients undergoing modified natural cycle during the IVF [6,76,77]. Furthermore, the

combined effect of both significant and non-significant deregulated levels of individual N-glycan species in FF led to more pronounced differences between analyzed FFNG profiles reflected through derived N-glycome features. Indeed, the analysis of the FFNGs-derived traits revealed 14 significantly deregulated traits between analyzed groups, which included additional features derived from the complex type N-glycan compositions (Figure 5 and Supplementary Table 6). The majority of observed differences were associated with diantennary compositions. In the MNC group, significantly increased fucosylation and galactosylation levels were observed in comparison with the COH group of patients (Figure 5 and Supplementary Table 6). This was accompanied by significantly increased levels of galactosylation and sialylation (including α 2,6-linked) of fucosylated diantennary compositions (Figure 5 and Supplementary Table 6). These type of the diantennary compositions most likely originate from FF IgA, IgM or Fab portions of the IgG [78]. The increase in these FFNG characteristics may also be indicative of the presence of local inflammatory responses [82], which correspond to the type of inflammation associated with normal ovulatory process [9]. Also, as no differences in FF immunoglobulins concentrations associated with different stimulation protocols were previously observed [79], we may propose that observed differences in immunoglobulin N-glycome features in this study may arise from differential glycosyltransferase activity. Indeed, glycosyltransferases' activity is known to be regulated in the antibody producing cells by various environmental factors, such as cytokine stimulation [83]. This hypothesis is consistent with the results of previous studies which have demonstrated that COH greatly affects intra-follicular and system cytokine networks [84]. On the other hand, in the COH group, we observed significantly increased levels of general and α 2,6-linked sialylated diantennary compositions as well. This was accompanied by significantly elevated levels of both types of sialylation on the level of afucosylated diantennary compositions in the COH group (Figure 5 and Supplementary Table 6). These types of compositions are most likely derived from the APP as α-1-antitrypsin, complement component C3, haptoglobin, transferrin and others [80], where elevated levels were detected in previous proteomic studies of FF obtained from patients undergoing GnRH Ant stimulations protocols [76,77]. Interestingly, similar N- glycosylation featured patterns observed in the FFNG of the COH group (i.e. increased agalactosylation and afucosylation of diantennary compositions) were previously reported in the total plasma N-glycomes of chronic inflammatory diseases, such as rheumatoid arthritis (RA) [85] and inflammatory bowel disease (IBD) [34], when compared to healthy controls. Additionally, in both RA and IBD TPNG profiles, lower levels of sialylated fucosylated diantenarry compositions (especially of the α 2,6- type in the IBD patients) were also observed in comparison to healthy controls. These observations are similar to our results which indicate a localised inflammatory response underlined by glycosylation features of chronic inflammation in the COH group of patients. Similarly, significantly increased galactosylation and fucosylation levels were also observed in the MNC vs. COH groups of patients for triantennary complex features derived from FFNGs. This was further accompanied by significantly increased galactosylation and specifically α 2,6- sialylation levels of fucosylated triantennary compositions, in the MNC group (Figure 5 and Supplementary Table 6). These type of compositions are usually linked to the APPs [46], and are associated with pro-inflammatory immune responses observed in various pathological conditions, in particular elevated fucosylation levels [86]. Moreover, increased fucosylation combined with elevated galactosylation of triantennary structures observed in the MNC group raises the possibility of the formation of pro-inflammatory Sialyl Lewis X type structure characteristics for an acute immune response [87]. This process requires fucosylation of outer antennae and linkage of sialic in α 2,3- position of triantennary or tetraantennary compositions [88]. Furthermore, this observation is also supported with a non-significant increase in fucosylated α 2,3- sialylated tetraantennary compositions observed in the MNC group as well (Supplementary Table 6). In line with this, increased α 2,6- sialylation levels of fucosylated triantennary compositions were previously positively associated with changes associated with acute immune response in patients suffering from lung cancer [89] and acute system inflammation in patients recovering after cardiac surgery [33]. Taking all this into account, we may propose that observed differences in FFNGs between MNC and COH group of patients clearly indicate a localised inflammatory response underlined by specific glycosylation features indicative for an acute inflammation in the MNC group, which is normally required for rapid tissue degradation and remodelling during normal ovulatory process [90]. On the other hand, the FFNG signatures of the COH group strongly resemble the plasma/serum N-glycome changes associated with chronic inflammatory processes, which may be attributed to the deregulated localized inflammatory response associated with biological processes involved in ruptures of multiple follicles during the GnRH Ant treatment.

In conclusion, a comprehensive MALDI-TOF-MS profiling of the FF IgG N-glycomes and FFNGs obtained from two set of patients that underwent IVF procedure by different stimulation protocols, suggest that the observed differences between FF IgG N-glycomes and FFNGs point to deregulated inflammatory processes associated with specific IVF stimulation protocol applied in patients. A research approach encompassing a larger sample set and focused on glycosylation analysis of a panel of individual FF APPs and immunoglobulins (including their subclasses), might additionally clarify the inflammatory mechanisms underlying different IVF stimulation protocols.

Conflict of interest: Authors state no conflict of interest

Authors' contributions: MK designed the N-glycan profiling experimental protocol and glycan assignment procedure, performed all MALDI-TOF-MS analyses and drafted the manuscript body as part of his postdoc; SDP and IC performed sample preparation and participated in manuscript writing; NSS and TM collected follicular fluid samples; NSS and SDP performed patient selection for research; NSS performed final revision of the manuscript in the clinical field; MK and SKP conceived and designed the project, analyzed and interpreted data, performed literature search, prepared corresponding tables and figures; SDP and ARB performed literature search in the clinical field and participated in writing of corresponding manuscript parts; SKP performed final write-up, literature check and revision of the manuscript. All authors discussed the complete set of results and commented on the manuscript.

References

1. Conti M, Franciosi F. Acquisition of oocyte competence to develop as an embryo: integrated nuclear and cytoplasmic events. Hum Reprod Update. 2018;24:245–66.

2. Santos-Ribeiro S, Mackens S, Racca A, Blockeel C. Towards complication-free assisted reproduction technology. Best Pract Res Clin Endocrinol Metab. 2019;33:9–19.

3. Dumesic DA, Meldrum DR, Katz-Jaffe MG, Krisher RL, Schoolcraft WB. Oocyte environment: follicular fluid and cumulus cells are critical for oocyte health. Fertil Steril. 2015;103:303–16.

4. Bianchi L, Gagliardi A, Landi C, Focarelli R, De Leo V, Luddi A, et al. Protein pathways working in human follicular fluid: the future for tailored IVF? Expert Rev Mol Med. 2016;18:e9.

5. Aghadavod E, Zarghami N, Farzadi L, Zare M, Barzegari A, Akbar Movassaghpour A, et al. Isolation of granulosa cells from follicular fluid; applications in biomedical and molecular biology experiments. Adv Biomed Res [Internet]. 2015 [cited 2020 Mar 3];4:250. Available from: https://www.ncbi.nlm.nih.gov/pmc/articles/PMC4746942/

6. Zamah AM, Hassis ME, Albertolle ME, Williams KE. Proteomic analysis of human follicular fluid from fertile women. Clin Proteomics. 2015;12:5.

7. Lehmann R, Schmidt A, Pastuschek J, Müller MM, Fritzsche A, Dieterle S, et al. Comparison of sample preparation techniques and data analysis for the LC-MS/MS-based identification of proteins in human follicular fluid. Am J Reprod Immunol. 2018;80:e12994.

8. Boots CE, Jungheim ES. Inflammation and human ovarian follicular dynamics. Semin Reprod Med. 2015;33:270–5.

9. Duffy DM, Ko C, Jo M, Brannstrom M, Curry TE. Ovulation: parallels with inflammatory processes. Endocr Rev. 2019;40:369–416.

10. Büscher U, Chen FC, Kentenich H, Schmiady H. Cytokines in the follicular fluid of stimulated and non-stimulated human ovaries; is ovulation a suppressed inflammatory reaction? Hum Reprod. 1999;14:162–6.

11. Sarapik A, Velthut A, Haller-Kikkatalo K, Faure GC, Béné MC, de Carvalho Bittencourt M, et al. Follicular proinflammatory cytokines and chemokines as markers of IVF success. Clin Dev Immunol. 2012;2012:606459.

12. Escobar-Morreale HF, Luque-Ramírez M, González F. Circulating inflammatory markers in polycystic ovary syndrome: a systematic review and metaanalysis. Fertil Steril. 2011;95(3):1048-1058. e1-2.

13. Robker RL, Wu LL, Yang X. Inflammatory pathways linking obesity and ovarian dysfunction. J Reprod Immunol. 2011;88:142–8.

14. Orvieto R. Controlled ovarian hyperstimulation—an inflammatory state. J Soc Gynecol Investig. 2004;11:424–6.

15. Orvieto R, Chen R, Ashkenazi J, Ben-Haroush A, Bar J, Fisch B. C-reactive protein levels in patients undergoing controlled ovarian hyperstimulation for IVF cycle. Hum Reprod. 2004;19(2):357–9.

16. Almagor M, Hazav A, Yaffe H. The levels of C-reactive protein in women treated by IVF. Hum Reprod. 2004;19:104–6.

17. Levin I, Gamzu R, Hasson Y, Lessing JB, Amit A, Shapira I, et al. Increased erythrocyte aggregation in ovarian hyperstimulation syndrome: a possible contributing factor in the pathophysiology of this disease. Hum Reprod. 2004;19(5):1076–80.

18. Levin I, Gamzu R, Pauzner D, Rogowski O, Shapira I, Maslovitz S, et al. Elevated levels of CRP in ovarian hyperstimulation syndrome: an unrecognised potential hazard? BJOG Int J Obstet Gynaecol. 2005;112(7):952–5.

19. Medzhitov R. Inflammation 2010: new adventures of an old flame. Cell. 2010;140:771–6.

20. Ohtsubo K, Marth JD. Glycosylation in cellular mechanisms of health and disease. Cell. 2006;126:855–67.

21. Gornik O, Lauc G. Glycosylation of serum proteins in inflammatory diseases. Dis Markers. 2008;25:267–78.

22. Wong CH. Protein glycosylation: new challenges and opportunities. J Org Chem. 2005;70:4219–25.

23. Gupta G, Surolia A. Glycomics: an overview of the complex glycocode. Adv Exp Med Biol. 2012;749:1–13.

24. Lauc G, Vojta A, Zoldoš V. Epigenetic regulation of glycosylation is the quantum mechanics of biology. Biochim Biophys Acta. 2014;1840:65–70.

25. Reily C, Stewart TJ, Renfrow MB, et al. Glycosylation in health and disease. Nat Rev Nephrol. 2019;15:346–66.

26. Tankeshwar A. Immunoglobulin G (IgG): structure, subclasses, functions and clinical significance. Learn Microbiol. Online [Internet]. 2018 Sep [cited 2020 Feb 27]. Available from: https://microbeonline.com/igg-antibody-structure-subclasses-functions-and-clinical-significance/

27. Vidarsson G, Dekkers G, Rispens T. IgG subclasses and allotypes: from structure to effector functions. Front Immunol. 2014;5:520.

28. van de Bovenkamp FS, Hafkenscheid L, Rispens T, Rombouts Y. The emerging importance of IgG Fab glycosylation in immunity. J Immunol. 2016;196(4):1435–41.

29. Alter G, Ottenhoff TH, Joosten SA. Antibody glycosylation in inflammation, disease and vaccination. Semin Immunol. 2018;39:102–10.

30. Li T, DiLillo DJ, Bournazos S, Giddens JP, Ravetch JV, Wang LX. Modulating IgG effector function by Fc glycan engineering. Proc Natl Acad Sci U S A. 2017;114(13):3485–90.

31. Kaneko Y, Nimmerjahn F, Ravetch JV. Anti-inflammatory activity of immunoglobulin G resulting from Fc sialylation. Science. 2006;313:670–3.

32. Pereira NA, Chan KF, Lin PC, Song Z. The "less-is-more" in therapeutic antibodies: afucosylated anti-cancer antibodies with enhanced antibody-dependent cellular cytotoxicity. MAbs. 2018;10(5):693–711.

33. Novokmet M, Lukić E, Vučković F, Đuric Ž, Keser T, Rajšl K, et al. Changes in IgG and total plasma protein glycomes in acute systemic inflammation. Sci Rep. 2014;4:4347.

34. Clerc F, Novokmet M, Dotz V, Reiding KR, de Haan N, Kammeijer GSM, et al. Plasma N-glycan signatures are associated with features of inflammatory bowel diseases. Gastroenterology. 2018;155(3):829–43.

35. Nargund G, Fauser BC, Macklon NS, Ombelet W, Nygren K, Frydman R, et al. The ISMAAR proposal on terminology for ovarian stimulation for IVF. Hum Reprod. 2007;22(11):2801–4.

36. Jansen BC, Bondt A, Reiding KR, Scherjon SA, Vidarsson G, Wuhrer M. MALDI-TOF-MS reveals differential N-linked plasma- and IgG-glycosylation profiles between mothers and their newborns. Sci Rep. 2016;6:34001.

37. Reiding KR, Blank D, Kuijper DM, Deelder AM, Wuhrer M. High-throughput profiling of protein N-glycosylation by MALDI-TOF-MS employing linkage-specific sialic acid esterification. Anal Chem. 2014;86(12):5784–93.

38. Selman MH, Hemayatkar M, Deelder AM, Wuhrer M. Cotton HILIC SPE microtips for microscale purification and enrichment of glycans and glycopeptides. Anal Chem. 2011;83(7):2492–9.

39. Cooper CA, Gasteiger E, Packer NH. GlycoMod—a software tool for determining glycosylation compositions from mass spectrometric data. Proteomics. 2001;1:340–9.

40. Varki A, Cummings RD, Aebi M, Packer NH, Seeberger PH, Esko JD, et al. Symbol nomenclature for graphical representations of glycans. Glycobiology. 2015;25(12):1323–4.

41. Imre T, Kremmer T, Héberger K, Molnár-Szöllősi É, Ludányi K, Pócsfalvi G, et al. Mass spectrometric and linear discriminant analysis of N-glycans of human serum alpha-1-acid glycoprotein in cancer patients and healthy individuals. J Proteomics. 2008;71(2):186–97.

42. de Vroome SW, Holst S, Girondo MR, van der Brugt YEM, Mesker ME, Tollenaar RAEM, et al. Serum N-glycome alterations in colorectal cancer associate with survival. Oncotarget. 2018;9(55):30610–23.

43. Dědová T, Braicu EI, Sehouli J, Blanchard V. Sialic acid linkage analysis refines the diagnosis of ovarian cancer. Front Oncol [Internet]. 2019 Apr [cited 2020 Mar 3];9:261 [about 11p.]. Available from: https://www.ncbi.nlm.nih.gov/pmc/articles/PMC6499200/pdf/fonc-09-00261.pdf

44. Russell A, Adua E, Ugrina I, Laws S, Wang W. Unravelling immunoglobulin G Fc N-glycosylation: a dynamic marker potentiating predictive, preventive and personalised medicine. Int J Mol Sci. [Internet]. 2018 Jan [cited 2020 Feb 27];19(2):390 [about 18 p.]. Available from: https://www.ncbi.nlm.nih.gov/pmc/articles/PMC5855612/

45. Schweigert FJ, Gericke B, Wolfram W, Kaisers U, Dudenhausen JW. Peptide and protein profiles in serum and follicular fluid of women undergoing IVF. Hum Reprod. 2006;21(11):2960–8.

46. Clerc F, Reiding KR, Jansen BC, Kammeijer GSM, Bondt A, Wuhrer M. Human plasma protein N-glycosylation. Glycoconj J. 2016;33:309–43.

47. Dotz V, Lemmers RF, Reiding KR, Hipgrave Ederveen AL, Lieverse AG, Mulder MT, et al. Plasma protein N-glycan signatures of type 2 diabetes. Biochim Biophys Acta Gen Subj. 2018;1862(12):2613–22.

48. Gebrehiwot AG, Melka DS, Kassaye YM, Gemechu T, Lako W, Hinou H, et al. Exploring serum and immunoglobulin G N-glycome as diagnostic biomarkers for early detection of breast cancer in Ethiopian women BMC Cancer [Internet].. 2019 Jun [cited 2020 Feb 27];19(1):588 [about 18 p.]. Available from: https://www.ncbi.nlm.nih.gov/pmc/articles/PMC6580580/

49. Huang C, Liu Y, Wu H, Sun D, Li Y. Characterization of IgG glycosylation in rheumatoid arthritis patients by MALDI-TOF-MSn and capillary electrophoresis. Anal Bioanal Chem. 2017;409(15):3731–9.

50. Orisaka M, Tajima K, Tsang BK, Kotsui F. Oocyte-granulosa-theca cell interactions during preantral follicular development. J Ovarian Res. 2009;2(1):9.

51. Espey LL. Current status of the hypothesis that mammalian ovulation is comparable to an Inflammatory reaction. Biol Reprod. 1994;50:233–8.

52. Kovacs P, Kovats T, Bernard A, Zadori J, Szmatona G, Kaali SG. Comparison of serum and follicular fluid hormone levels with recombinant and urinary human chorionic gonadotropin during in vitro fertilization. Fertil Steril. 2008;90(6):2133–7.

53. Schenker JG, Weinstein D. Ovarian hyperstimulation syndrome: a current survey. Fertil Steril. 1978;30:255–68.

54. Shen X, Liu X, Zhu P, Zhang Y, Wang J, Wang Y, et al. Proteomic analysis of human follicular fluid associated with successful in vitro fertilization. Reprod Biol Endocrinol. 2017;15(1):58.

55. Nayudu PL, Lopata A, Jones GM, Gook DA, Bourne HM, Sheather SJ, et al. An analysis of human oocytes and follicles from stimulated cycles: oocyte morphology and associated follicular fluid characteristics. Hum Reprod. 1989;4(5):558–67.

56. Lamb JD, Zamah AM, Shen S, McCulloch C, Cedars MI, Rosen MP. Follicular fluid steroid hormone levels are associated with fertilization outcome after intracytoplasmic sperm injection. Fertil Steril. 2010;94(3):952–7.

57. Wu YM, Nowack DD, Omenn GS, Haab BB. Mucin glycosylation is altered by pro-inflammatory signaling in pancreatic-cancer cells. J Proteome Res. 2009;8(4):1876–86.

58. Miller DL, Jones CJ, Aplin JD, Nardo LG. Altered glycosylation in peri-implantation phase endometrium in women with stages III and IV endometriosis. Hum Reprod. 2010;25(2):406–11.

59. Bondt A, Rombouts Y, Selman MH, Hensbergen PJ, Reiding KR, Hazes JMW, et al. Immunoglobulin G (IgG) Fab glycosylation analysis using a new mass spectrometric high-throughput profiling method reveals pregnancy-associated changes. Mol Cell Proteomics. 2014;13(11):3029–39.

60. Vučković F, Krištić J, Gudelj I, Teruel M, Keser T, Pezer M, et al. Association of systemic lupus erythematosus with decreased immunosuppressive potential of the IgG glycome. Arthritis Rheumatol. 2015;67(11):2978–89.

61. Clarke GN, Hsieh C, Koh SH, Cauchi MN. Sperm antibodies, immunoglobulins, and complement in human follicular fluid. Am J Reprod Immunol Am J Immunol. 1984;5(4):179–81.

62. de Haan N, Boeddha NP, Ekinci E, Reiding KR, Emonts M, Hazelzet JA, et al. Differences in IgG Fc glycosylation are associated with outcome of pediatric meningococcal sepsis. MBio [Internet]. 2018 May-Jun [cited 2020 Feb 27];9(3): e00546-18 [about 13 p.]. Available from: https://www.ncbi.nlm.nih.gov/pmc/articles/PMC6016251/pdf/mBio.00546-18.pdf

63. Rodgers RJ, Irving-Rodgers HF. Formation of the ovarian follicular antrum and follicular fluid. Biol Reprod. 2010;82:1021–9.

64. Ghirardello A, Gizzo S, Noventa M, Quaranta M, Vitagliano A, Gallo N, et al. Acute immunomodulatory changes during controlled ovarian stimulation: evidence from the first trial investigating the short-term effects of estradiol on biomarkers and B cells involved in autoimmunity. J Assist Reprod Genet. 2015;32(12):1765–72.

65. Ullah K, Rahman TU, Pan HT, Guo MX, Dong XY, Liu J, et al. Serum estradiol levels in controlled ovarian stimulation directly affect the endometrium. J Mol Endocrinol. 2017;59(2):105–19.

66. Engdahl C, Bondt A, Harre U, Raufer J, Pfeifle R, Camponeschi A, et al. Estrogen induces St6gal1 expression and increases IgG sialylation in mice and patients with rheumatoid arthritis: a potential explanation for the increased risk of rheumatoid arthritis in postmenopausal women. Arthritis Res Ther. 2018;20(1):84.

67. Ercan A, Kohrt WM, Cui J, Deane KD, Pezer M, Yu EW, et al. Estrogens regulate glycosylation of IgG in women and men. JCI Insight [Internet]. 2017 Feb [cited 2020 Feb 27];2(4):e89703 [about 10 p.]. Available from: https://insight.jci.org/articles/view/89703/pdf

68. Bondt A, Selman MH, Hazes JM, Deelder AM, Wuhrer M, Dolhain RJEM. Changes in IgG-Fc N-glycan sialylation, galactosylation and fucosylation influence disease activity during and after pregnancy in rheumatoid arthritis. Ann Rheum Dis. 2012;71(Suppl 1):A34–5.

69. Gudelj I, Lauc G, Pezer M. Immunoglobulin G glycosylation in aging and diseases. Cell Immunol. 2018;333:65–79.

70. Nimmerjahn F, Anthony RM, Ravetch JV. Agalactosylated IgG antibodies depend on cellular Fc receptors for in vivo activity. Proc Natl Acad Sci USA. 2007;104:8433–7.

71. Plomp R, Ruhaak LR, Uh HW, Reiding KR, Selman M, Houwing-Duistermaat JJ, et al. Subclass-specific IgG glycosylation is associated with markers of inflammation and metabolic health. Sci Rep. 2017;7: 12325.

72. Shade KT, Anthony RM. Antibody glycosylation and inflammation. Antibodies (Basel). 2013;2:392–414.

73. Dekkers G, Treffers L, Plomp R, Bentlage AEH, de Boer M, Koeleman CAM, et al. Decoding the human immunoglobulin G-glycan repertoire reveals a spectrum of Fc-receptor- and complement-mediated-effector activities. Front Immunol. 2017;8:877.

74. Peschke B, Keller CW, Weber P, Quast I, Lünemann JD. Fc-galactosylation of human Immunoglobulin gamma Isotypes Improves C1q binding and enhances complement-dependent cytotoxicity. Front Immunol. 2017;8:646.

75. Kushnir MM, Naessén T, Wanggren K, Rockwood AL, Crockett DK, Bergquist J. Protein and steroid profiles in follicular fluid after ovarian hyperstimulation as potential biomarkers of IVF outcome. J Proteome Res. 2012;11(10):5090–100.

76. Wu YT, Wu Y, Zhang JY, Hou NN, Liu AX, Pan JX, et al. Preliminary proteomic analysis on the alterations in follicular fluid proteins from women undergoing natural cycles or controlled ovarian hyperstimulation. J Assist Reprod Genet. 2015;32(3):417–27.

77. Lim HJ, Seok AE, Han J, Lee J, Lee S, Kang HG, et al. N-glycoproteomic analysis of human follicular fluid during natural and stimulated cycles in patients undergoing in vitro fertilization. Clin Exp Reprod Med. 2017;44(2):63–72.

78. Suhre K, Trbojević-Akmačić I, Ugrina I, Mook-Kanamori DO, Spector T, Graumann J, et al. Fine-Mapping of the Human Blood Plasma N-Glycome onto Its Proteome. Metabolites [Internet]. 2019 Jun [cited 2020 Feb 27];9(7):122 [about 13p.]. Available from: https://www.ncbi.nlm.nih.gov/pmc/articles/PMC6681129/

79. Hammadeh ME, Ertan AK, Zeppezauer M, Baltes S, Georg T, Rosenbaum P, et al. Immunoglobulins and cytokines level in follicular fluid in relation to etiology of infertility and their relevance to IVF outcome. Am J Reprod Immunol. 2002;47(2):82–90.

80. Chatterjee BP, Mondal G, Chatterjee U. Glycosylation of acute phase proteins: a promising disease biomarker. Proc Natl Acad Sci, India, Sect B Biol Sci. 2014;84:865–74.

81. Angelucci S, Ciavardelli D, Di Giuseppe F, Eleuterio E, Sulpizio M, Tiboni GM, et al. Proteome analysis of human follicular fluid. Biochim Biophys Acta. 2006;1764(11):1775–85.

82. Ferrantelli E, Farhat K, Ederveen AL, Reiding KR, Beelen RHJ, van Ittersum FJ, et al. Effluent and serum protein N-glycosylation is associated with inflammation and peritoneal membrane transport characteristics in peritoneal dialysis patients. Sci Rep. 2018;8(1):979.

83. Wang J, Balog CIA, Stavenhagen K, Koeleman CAM, Scherer HU, Selman MHJ, et al. Fc-glycosylation of IgG1 is modulated by B-cell stimuli. Mol Cell Proteomics. 2011;10(5):M110.004655.

84. Baskind NE, Orsi NM, Sharma V. Impact of Exogenous Gonadotropin Stimulation on Circulatory and Follicular Fluid Cytokine Profiles. Int J Reprod Med [Internet]. 2014 [cited 2020 Feb 28];2014:218769 [about 11 p.]. Available from: https://www.ncbi.nlm.nih.gov/pmc/articles/PMC4334052/

85. Reiding KR, Vreeker GC, Bondt A, Bladergroen MR, Hazes JMW, van der Burgt YEM, et al. Serum protein N-glycosylation changes with rheumatoid arthritis disease activity during and after pregnancy. Front Med. 2017;4:241.

86. McCarthy C, Saldova R, Wormald MR, Rudd PM, McElvaney NG, Reeves EP, et al. The role and importance of glycosylation of acute phase proteins with focus on alpha-1 antitrypsin in acute and chronic inflammatory conditions. J Proteome Res. 2014;13(7):3131–43.

87. De Graaf TW, Van der Stelt ME, Anbergen MG, van Diijk W. Inflammation-induced expression of sialyl Lewis X-containing glycan structures on alpha 1-acid glycoprotein (orosomucoid) in human sera. J Exp Med. 1993;177(3):657–66.

88. Trinchera M, Aronica A, Dall'Olio F. Selectin Ligands Sialyl-Lewis a and Sialyl-Lewis x in Gastrointestinal Cancers. Biology (Basel) [Internet]. 2017 Mar [cited 2020 Feb 28];6(1):16 [about 18 p.]. Available from: https://www.ncbi.nlm.nih.gov/pmc/articles/PMC5372009/pdf/biology-06-00016.pdf

89. Vasseur JA, Goetz JA, Alley WR, Novotny MV. Smoking and lung cancer-induced changes in N-glycosylation of blood serum proteins. Glycobiology. 2012;22(12):1684–708.

90. Tsafriri A. Ovulation as a Tissue Remodelling Process. In: Mukhopadhyay AK, Raizada MK, editors. Tissue Renin-Angiotensin Syst Curr Concepts Local Regul Reprod Endocr Organs. Boston: Springer US; 1995. p. 121–40.